Subband Analysis and Synthesis of Volumetric Medical Images Using Wavelet*

Chang Wen Chen,† Ya-Qin Zhang‡, Kevin J. Parker†

†Department of Electrical Engineering
University of Rochester
Rochester, NY 14627

‡GTE Laboratories
40 Sylvan Road
Waltham, MA 02254

ABSTRACT

We present in this paper a study of subband analysis and synthesis of volumetric medical images using 3D separable wavelet transforms. With 3D wavelet decomposition, we are able to investigate the image features at different scale levels that correspond to certain characteristics of biomedical structures contained in the volumetric images. The volumetric medical images are decomposed using 3D wavelet transforms to form a multi–resolution pyramid of octree structure. We employ a 15–subband decomposition in this study, where band 1 represents the subsampled original volumetric images and other subbands represent various high frequency components of a given image. Using the available knowledge of the characteristics of various medical images, an adaptive quantization algorithm based on clustering with spatial constraints is developed. Such adaptive quantization enables us to represent the high frequency subbands at low bit rate without losing clinically useful information. The preliminary results of analysis and synthesis show that, by combining the wavelet decomposition with the adaptive quantization, the volumetric biomedical images can be coded at low bit rate while still preserving the desired details of biomedical structures.

Keywords: Subband coding, wavelet, volumetric medical images, adaptive quantization, Gibbs random field

1. INTRODUCTION

The rapid development of 3D and 4D medical imaging techniques has produced tremendous amount of medical image data that can overwhelm the storage and transmission capabilities of conventional archiving systems. Image compression has now become mandatory for various medical picture archiving and communication systems. Unlike other image compression applications, compression of medical images is usually required to be lossless. However, lossless compression techniques often provide inadequate compression ratios for many types of medical image coding applications. The lossy compression techniques are acceptable for medical applications only if the clinical useful information can be preserved in the encoding and decoding processes [1]. We present in this paper the study of subband analysis and synthesis of volumetric medical images using 3D separable wavelet transforms. With the proposed 3D wavelet decomposition and an adaptive quantization scheme, the volumetric medical images can be coded at low bit rate while still preserving the desired details of biomedical structures.

Recently, the wavelet transform has been successfully applied to subband image and video coding applications [2, 3, 4, 5]. The excellent localization in both spatial and frequency domains have made the application of wavelet an ideal choice to the analysis and synthesis of various medical images . In this research,

* This research was supported by NSF Grant EEC-92-09615 and a New York State Science and Technology Foundation Grant to the Center for Electronic Imaging Systems at the University of Rochester.

0-8194-1638-X/94/$6.00

the volumetric medical images are decomposed using 3D wavelet transforms to form a multi–resolution pyramid of octree structure (in contrast to quadtree structure in 2D case). We employ a 15–subband decomposition in this study, where band 1 represents the subsampled original volumetric images and other subbands represent various high frequency components of the given image. The wavelet decomposition of the volumetric image provides us a hierarchical structure of subimages whose features correspond to the biomedical structures at different levels. Such decomposition enables us to identify the characteristics of the volumetric image at different scale levels and enable the design of a quantization algorithm suitable for lower bit rate for coding.

Our adaptive quantization algorithm is based on K-means clustering with spatial constraints modeled by the Gibbs random field [6, 7]. This quantization algorithm is different from conventional scalar or vector quantizations in that a pixel is quantized according to two criteria: (1) its gray level, and (2) its neighborhood information. The neighborhood spatial constraints provide us a flexible and powerful tool for quantization of high frequency subbands. High frequency subbands usually are sparse and highly structured, but many isolated impulse like pixels, generally of negligible visual significance, often need considerable bits to code. With spatial constraints, these impulse like pixels are forced to be clustered as the same class as its neighbors. The parameters of the Gibbs random field can be related to the medical structures in the images and therefore can be specified by the available anatomical knowledge of given images. In particular, we have made use of the relative size of the biomedical structures in order to enforce a reasonable spatial constraint so that no useful biomedical information is removed in the process of clustering. A great reduction of entropy is obtained after the constrained adaptive quantization has been applied to the high frequency subbands. The reduction of entropy indicates that efficient coding schemes can be designed for these sparse and well structured subbands.

The 3D subband synthesis based on the original base band and the quantized high frequency bands has also been conducted. The synthesized image illustrated that a high quality reconstruction can be obtained from the reduced entropy high frequency subbands. In particular, the clinical useful information can be preserved if the parameters of the Gibbs random field are chosen appropriately according to the available knowledge of the biomedical structures.

The proposed analysis and synthesis approach has been applied to a set of volumetric MR brain images. The preliminary results of analysis and synthesis using 3D wavelet decomposition and adaptive quantization with spatial constraints suggest that the volumetric biomedical images can be coded at low bit rate without losing clinically significant visual information.

2. SUBBAND ANALYSIS AND SYNTHESIS OF 3D IMAGES USING WAVELET

Subband coding was initially developed for speech coding by Crochiere in 1976 [8], and has since proved to be a powerful technique for both speech and image compression. The basic principle of subband coding is to decompose the signal spectrum into several frequency bands, and then code and transmit each band separately. The extension of the subband coding to multidimensional signal processing was introduced in [9] and the application for image and video compression has been attempted with much success [10, 11, 12]. In image coding applications, the subband decomposition is accomplished by passing the image data through a bank of bandpass analysis filters. Since the bandwidth of each filtered version of the image data is reduced, they can be subsampled at its new Nyquist frequency, resulting a series of reduced size subband images. Each subband image can then be coded, transmitted over the communication system, and decoded at the destination. These received subband images are then upsampled to form images of original size, and passed through the corresponding bank of synthesis filters, where they are interpolated and added to obtain the reconstructed image.

3D subband coding was originally proposed in [13] as a promising technique for video compression. With separable filters, 3D analysis and synthesis are carried out as a cascade of temporal, spatial horizontal, and spatial vertical unidirectional filters in a tree structural manner. Such cascade of filtering may be repeated for certain frequency subbands in order to achieve high compression rate. Important advantages of 3D subband coding include the low computational complexity and easy parallel implementation [13, 14].

In the following, a procedure for the decomposition of volumetric images by the 3D subband scheme is described. The volumetric decomposition of images is accomplished by passing the 3D image data through the same wavelet filter in horizontal, vertical, and normal directions, respectively. This is different from the scheme used to decompose video signals where the filter bank used for temporal decomposition is usually different from the filter bank used for spatial decompositions. In contrast to the quadtree structure in 2D decomposition, the volumetric subband decomposition results in a multi–resolution pyramid of octree structure. The analysis and synthesis are carried out according to the structure of octree decompositions.

2.1. Octree Decomposition of Volumetric Subband

In video signal coding, the temporal decomposition is usually based on the 2–tap Haar filterbank [3, 13] and results in a 11–band 2D subband structure. Such decomposition of video signals is not of true 3D characteristics since the lowpass and highpass 2–tap Haar filterings are basically the average and difference operations.

We propose a true 3D decomposition of volumetric image data which results in 15–band octree structure. The original volumetric image set is passed through a bank of unidirectional bandpass filters respectively so that the bandwidth of the resultant filtered image set is reduced. The filtered image set can now be subsampled along the filtering direction at its new Nyquist frequency, obtaining a series of reduced size subband image sets. In the case of volumetric image decomposition using two subbands along each direction, one cycle of horizontal, vertical, and normal flittering produces 8 subbands (LLL, LLH, HLL, HLH, LHL, LHH, HHL, HHH) of octree structure. Upon one cycle of decomposition, the lowest frequency subband may be further decomposed in the same fashion. Figure 1 shows a 15–band octree structure decomposition for volumetric image set in which the lowest frequency subband after first cycle is further decomposed.

In general, the type and length of the filters can be the same for all three spatial directions. However, in the case of medical images, the filters applied to each direction may be different considering that the physical resolutions along different directions are often different for a given set of volumetric image data. For example, many medical images are composed of a stack of 2D images in which the resolution between the stacks is not as high as the pixel resolution within the 2D images. A different filter with appropriate type and length may be used for the decomposition along the normal direction, or the direction of stacking. Such variation of filter selection is analogous to subband video coding in which the temporal filters are different from spatial filters.

2.2. Subband Analysis and Synthesis Using Wavelet

Subband analysis and synthesis of signals can be accomplished by the application of various filters, including quadrature mirror filterbanks, IIR filterbanks, and FIR filterbanks. With separable filters, 3D analysis and synthesis are carried out in a cascade fashion on each spatial direction. With the decomposition of octree structure, the analysis generates high frequency subbands containing horizontal, vertical, normal, and mixed diagonal high pass energy appeared as directional edges. To minimize the distortions caused by filtering, the filters are often required capable of perfect reconstruction. In practice, the perfect reconstruction is defined such that the reconstructed signal after synthesis is a perfect replica of the input signal, in the absence of

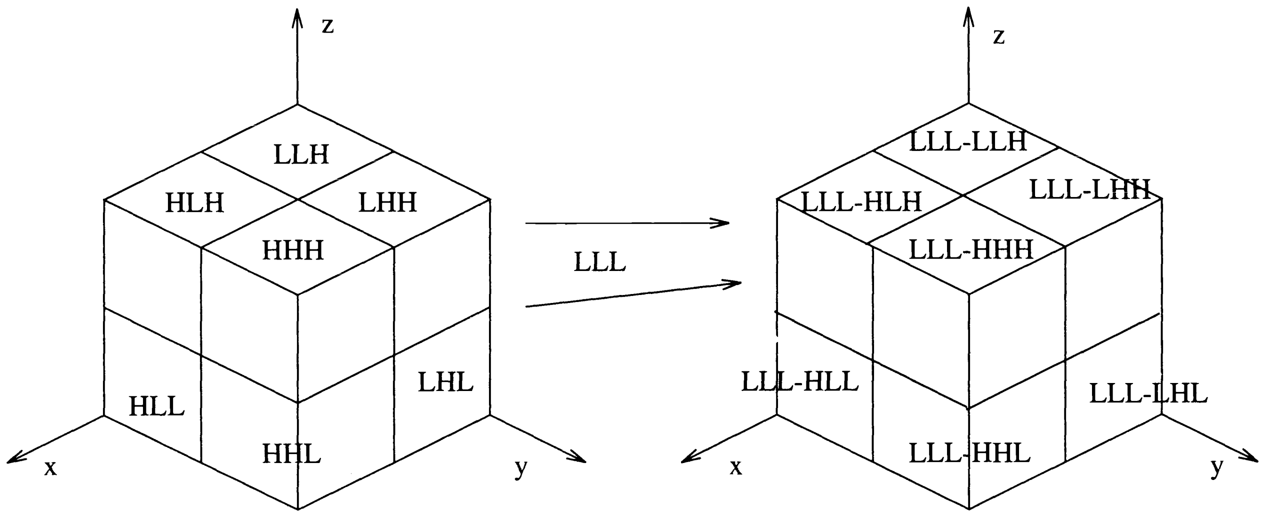

First level decompostion

Second level decomposition

Figure 1: A two-level octree structure of the subband decomposition of a volumetric image. The LLL subband and LLL-LLL subband cannot be labeled due to occlusion.

coding and transmission loss, with certain delay. Such perfect reconstruction condition can be written as:

$$\hat{X}(z) = z^{-k}X(z), \qquad k \in N \tag{1}$$

where $X(z)$ denotes the original signal, $\hat{X}(z)$ the synthesized signal, and k the delay.

In this research, wavelet filter is applied to decompose and reconstruct the volumetric medical images. It has been shown in [4, 5] that the wavelet transform corresponds well to the human psychovisual mechanism because of its localization features in both space and frequency domains. Moreover, the regularity and orthogonality of wavelet bases enable the reconstruction of medical images with high visual quality at very low bit-rate. The specific filters used in this research are an example of biorthogonal wavelet bases [5]. The lowpass analysis and synthesis filters can be expressed as:

$$H_l(z) = \frac{1}{\sqrt{2}}\sum_n h_n z^{-n} \qquad \text{and} \qquad G_l(z) = \frac{1}{\sqrt{2}}\sum_n g_n z^{-n} \tag{2}$$

where,

$$(h_0, h_{\pm 1}, h_{\pm 2}) = \left(\frac{3}{5}, \frac{1}{4}, -\frac{1}{20}\right) \tag{3}$$

and

$$(g_0,\ g_{\pm 1},\ g_{\pm 2},\ g_{\pm 3}) = \left(\frac{17}{28}, \frac{73}{280}, -\frac{3}{56}, -\frac{3}{280}\right). \tag{4}$$

If the highpass analysis and synthesis filters are written as:

$$H_h(z) = \frac{1}{\sqrt{2}}\sum_n \tilde{h}_n z^{-n} \qquad \text{and} \qquad G_h(z) = \frac{1}{\sqrt{2}}\sum_n \tilde{g}_n z^{-n}, \tag{5}$$

then, their coefficients are related to those of the lowpass analysis and synthesis filters under following constraints:

$$\begin{aligned} \tilde{g}_n &= (-1)^n h_{-n+1} \\ \tilde{h}_n &= (-1)^n g_{-n+1} \\ \sum_n h_n g_{n+2k} &= \delta_{k,0} \end{aligned} \tag{6}$$

to ensure the perfect reconstruction.

3. CHARACTERISTICS OF THE SUBBAND DECOMPOSITION

The subband analysis has not resulted in any reduction of bit rate required to represent the video signal. However, such analysis yields a desired decomposition of spatial spectrums into several frequency subbands. Through exploiting the characteristics of the decomposed subbands, an effective image coding algorithm can then be developed to represent the volumetric medical images at low bit rate without losing clinical useful information. Since the decomposed subbands exhibit quite different frequency responses from one to another, the coding strategy for each of them need to be carefully designed to fit individualized requirement in reducing the bit rate.

3.1. General Characteristics of the Decomposed Subbands

For the 15–band octree decomposition of the volumetric medical images, the characteristics of each band is summarized as follows:

1. Band 1 is the low resolution representation of the original image and has similar characteristics in histogram, but its bandwidth has been significantly reduced. For the 2–level decomposition to generate the octree structure, the bandwidth is only $\frac{1}{2^2}$ of the original bandwidth for each direction, thus its sampling rate requirement is reduced by same factor. It can be efficiently coded using DPCM since the lowpass filtered image is fairly smooth already. Block DCT coding is also expected to perform well for such band-limited image signal.
2. Bands 2-14 contain certain high frequency components of the volumetric images. Each image of these bands is highly structured and composed of different amount of "edges" and "impulses" corresponding to the features of original image at different scales and the directions of analysis filters. In particular, bands 2–7 usually contain more energy than the rest of them, and would need more bits to represent.
3. Band 15 represent all three spatial high frequency components of the volumetric images. It usually contains very low signal energy and is less significant than the rest. It can be discarded during the coding without visible distortions.

3.2. Representation of High Frequency Subbands

The design of an efficient coding algorithm utilizing the features of the decomposed subbands has been recognized as an effective way of increasing the compression ratio. In particular, many attempts in low bit rate subband coding have been concentrated in the study of characteristics of the high frequency subbands so that the features of these subbands can be made useful in designing low bit rate coding algorithms [3, 15, 16, 17]. When the decomposition is accomplished by the separable wavelet filters, the high frequency subbands exhibit excellent directionally localized structures which can be exploited to generate efficient representation.

Several features of these subbands should be taken into consideration for an efficient representation. One feature of these high frequency subbands is their less significant perceptual responses and hence can often afford coarse quantizations. Such coarse quantization would result in less bits to code the image with negligible distortions in the synthesized images. Another feature of the high frequency subbands is their well defined structures corresponding to properties of the bandpass filters. The structure of high frequency subbands usually appear as sparse "edges" and "impulses" that correspond to few strong discontinuities of the intensity changes along respective spatial directions. When the wavelet filters are used to decompose the volumetric image, the simultaneous localization in both frequency and spatial domains produces "edges" and "impulses" with even better contrast. In addition, these sparse "edges" and "impulses" exhibit their well defined directional arrangement in accordance with the direction of the filters applied to obtain these subbands. Utilization of such directional feature has been proposed in [18] that resulted in corresponding scanning scheme for runlength coding of subbands at different directions.

In the case of medical images, the strong edges with certain spatial extent in the decomposed high frequency subbands usually correspond to the biomedical structural patterns of clinical significance. However, the weak edges and impulses are often resulted from the noise or negligible image discontinuity patterns. It is evident that the quantization of these high frequency subbands should be designed such that the strong edges with certain spatial extent should be preserved while the weak edges and impulses should be merged with their neighbors. Unfortunately, traditional quantization schemes, either scalar quantization or vector quantization, would not be able to achieve this goal. This is because the scalar quantization does not recognize whether the given pixel is of impulse nature while vector quantization need a codebook generated before hand by training which would not adapt to the given signal. Therefore, an adaptive quantization scheme capable of identifying the spatial extent of an edge should be applied to these high frequency subbands to obtain the desired quantization.

4. ADAPTIVE QUANTIZATION WITH SPATIAL CONSTRAINTS

We propose here a novel approach for the adaptive quantization of high frequency subbands based on the concept of K-means clustering with spatial constraints. Our approach uses the Gibbs random field to enforce neighborhood constraints in order to remove those "impulses" whose contributions to the reconstruction are negligible, but would otherwise need considerable amount of bits to code. In the following, the adaptive clustering algorithm applied to high frequency subbands as an adaptive quantization is described and the implementation of this estimation algorithm as well as the selection of parameters are discussed.

4.1. Adaptive Clustering with Gibbs Random Field Model

The adaptive clustering algorithm with spatial constraints is applied to the high frequency subbands to obtain the desired quantization. This algorithm is a 3D extension of the K-means clustering scheme proposed in [6] with enhanced adaptability. It has been shown in [7, 19, 20] that images can be modeled as a Gibbs random field and image segmentation, or clustering of image pixels, can be accomplished through a maximum *a posteriori* probability (MAP) estimation technique. According to Bayes' theorem, the posterior probability can be expressed as:

$$p(x|y) \propto p(y|x)\, p(x) \tag{7}$$

where $p(x)$ is the *a priori* probability of the clustering, and $p(y|x)$ represents the conditional probability of the image data given the clustering. The Gibbs random field can be characterized by a neighborhood system and a potential function. A Gibbs random fields constrained image clustering is accomplished by assigning labels to each pixel in the given image. A label $x_s = i$ implies that the pixel s belongs to the i-th class of the K classes. Therefore, we have:

$$p(x_s|x_t, \quad \forall t \neq s) = p(x_s|x_t, \quad t \in N_s) \tag{8}$$

where N_s represents the defined neighborhood for pixel s. Associated with each neighborhood system are cliques and their potentials. A clique C is a set of sites where all elements are neighbors. If we consider that a 2D image is defined on the Cartesian grid and the neighborhood of a pixel is represented by its 4 nearest pixels [21], then the two-point clique potentials are defined as:

$$V_C(x) = \begin{cases} \beta, & \text{if } x_s = x_t \text{ and } s,t \in C \\ -\beta, & \text{if } x_s \neq x_t \text{ and } s,t \in C \end{cases} \tag{9}$$

For a 3D image, a straightforward extension of 2D neighborhood system indicates that the neighborhood a voxel can be represented by its 6 nearest neighbors [22]. A Gibbs distribution can then be defined as:

$$p(x) \propto \exp\left\{-\sum_C V_C(x)\right\} \tag{10}$$

where V_C is a certain clique potential for clique C. For a 4×4×4 3D lattice, there will be 24 cliques within each 4×4 cross section, and 16 cliques between two cross sections. The total number of two-point cliques for such 3D lattice is therefore 144. If we model the conditional density as a Gaussian process with mean μ_s and variance σ_s at a pixel location s, then it can be written as a spatial varying density function with respect to pixel location s:

$$p(y|x) \propto \exp\left\{-\sum_s \frac{1}{2\sigma_s^2}(y_s - \mu_s)^2\right\} \tag{11}$$

Then, the overall probability function will be:

$$p(x) \propto \exp\left\{-\sum_s \frac{1}{2\sigma_s^2}(y_s - \mu_s)^2 - \sum_C V_C(x)\right\} \tag{12}$$

There are two components in the overall probability function. One corresponds to the adaptive capability that force the clustering to be consistent with local image distribution with locally estimated mean μ_s and variance σ_s. The other corresponds to the spatial continuity constraint characterized by the clique potentials within a given 3D lattice.

4.2. Implementation of the Adaptive Quantization

MAP estimation based adaptive K-means clustering can be implemented using various optimization techniques depending on the specific applications. The proposed adaptive clustering algorithm for the quantization of high frequency subbands is implemented using the method of *iterative conditional mode* [23]. First, an initial clustering x is obtained through the simple K-means algorithm. Then, overall probability function is maximized on a point-by-point basis, with the mean μ_s and the variance σ_s of each cluster being updated after each iteration. Therefore, the optimization is accomplished through alternating between MAP estimation of the clustered regions and iterative update of the cluster means and variances. Such alternating process is repeated until no pixels change classes. The result is the optimal clustering of the given high frequency subbands.

The parameters in this adaptive clustering are chosen according to the characteristic of the high frequency subbands. Different β's are used for different directions when the clustering is applied to those subbands with clear directional edges while single β is used when the clustering is applied to subbands with no strong directional edges. Such flexible choice of parameters allows us to preserve those strong edges which often represent certain clinically useful information.

With Gibbs random field as the spatial constraint, the adaptive clustering algorithm is applied to obtain 5 levels of quantization with the gray level of each pixel being replaced by the mean of the cluster that pixel belongs to. Since the histogram of the high frequency subbands is approximately of Laplacian distribution with zero mean, the quantization levels are almost symmetrically distributed with the middle one close to zero. For display purpose, the zero valued mean is represented by the midgrey gray level, while negatively valued means are represented by dark gray levels and positively valued means are represented by bright gray levels.

5. PRELIMINARY RESULTS WITH VOLUMETRIC MR BRAIN IMAGES

The proposed scheme for subband analysis and synthesis of volumetric medical images has been applied to 3D MR brain images. The MR image data set is provided by the Department of Neurology, University of Rochester Medical Center. The MR imaging is performed using a GE Signa 1.5 Tesla superconducting system. This MR image set contains 60 slices, each with a matrix of 256×256 pixels. A typical slice from this brain image set is shown at the left of the Figure 2.

The given image volume is passed through a combination of highpass and lowpass wavelet filters along the horizontal, vertical, and normal directions, respectively. The filtered image volume is then subsampled at each directions to generate a smaller volume ($\frac{1}{8}$ of the original). All eight smaller volumes are arranged according to their frequency components as shown in Figure 1. The resultant LLL subband is further decomposed in the same fashion to generate a total of 15 subbands.

Band 1 is the low resolution representation of the original image with a significantly reduced bandwidth due to the two cycles of lowpass filtering. The subsequent adaptive quantization based on K-means clustering is not applied to band 1 since it contains no high frequency components. However, it is applied to the rest of the subbands to remove the impulses that are of insignificant visual importance, but would otherwise need considerable amount of bits to code. By a proper choice of spatial constraint parameters, the clinical useful information can be preserved during the process of adaptive quantization. Figure 3 shows one representative slice of the decomposed subbands from the octree structured volume before and after adaptive quantization. It is evident that the clinical useful information is preserved after adaptive quantization. However, the impulse, or edges with negligible spatial extent, have been largely removed. The image after adaptive quantization contains much more homogeneous regions than the corresponding original decomposition. A comparison of different order of entropy for each subband before and after adaptive quantization is presented in Table 1. This comparison indicates that an average reduction of entropy is about 70%. Therefore, the quantized subbands can be coded at much lower bit rate than the original subbands.

The synthesis is also accomplished using wavelet transforms. In the case of 2–level decomposition, we start from the LLL subband, where each subband in the second level decomposition of the octree structure is upsampled and passed through the corresponding synthesis filter. Upon the completion of the LLL subband synthesis, the first level octree structure is processed in the same fashion. We have obtained the synthesized volumetric image based on the original base band and the quantized high frequency subbands processed by adaptive clustering. The preliminary results show that a good quality image can be synthesized in this fashion but the adaptively quantized high frequency subbands can be represented at much lower bit rate. A typical slice after synthesis is shown at the right of the Figure 2 with PSNR of approximately 30dB. Visual inspection also shows that useful biomedical structures at various spatial levels are preserved. In particular, the detail of strong and clinically important structures remain the same while the noise contained in the given image has been suppressed.

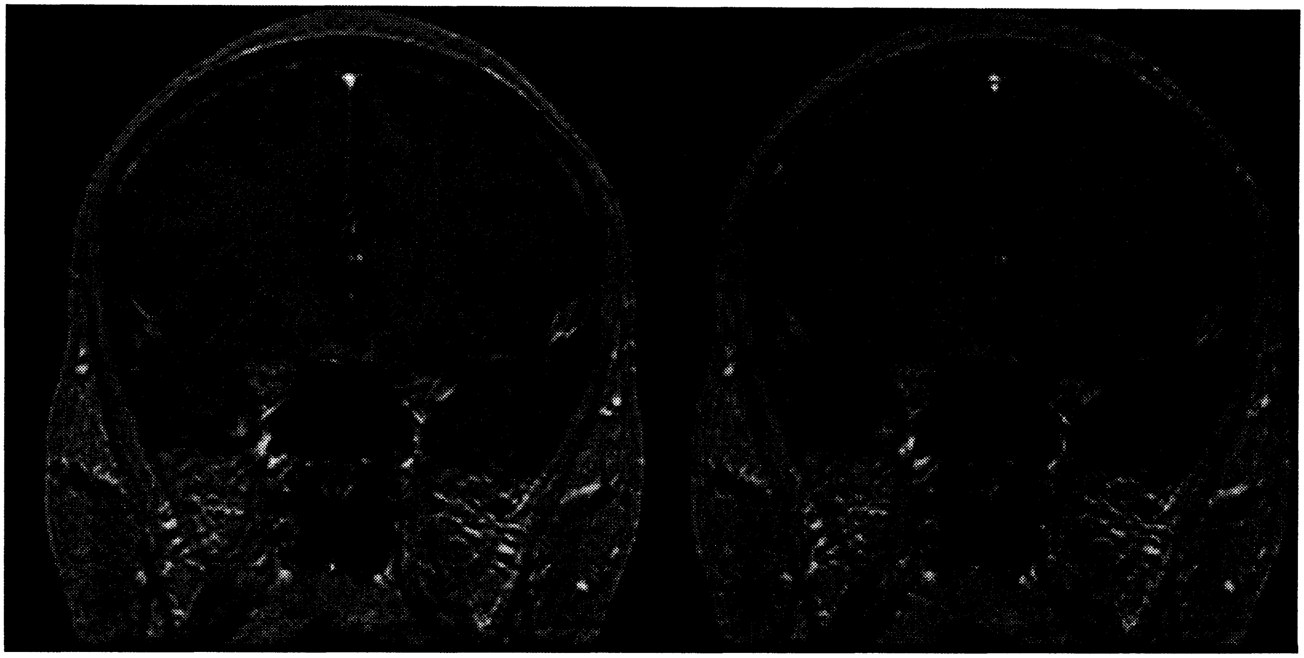

Figure 2: Left: A typical slice of brain image (slice 48) from the original volume; Right: The resultant image obtained after synthesis with the adaptively quantized subbands.

6. CONCLUSION

We have presented in this paper a study of subband analysis and synthesis of volumetric medical images using 3D separable wavelet transforms. With 3D wavelet decomposition, we are able to investigate the image features at different scale levels that correspond to certain characteristics of biomedical structures contained in the volumetric images. The volumetric medical image is decomposed into a 15–subband multi–resolution pyramid of octree structure. Using the available knowledge of the characteristics of various medical images, an adaptive quantization algorithm based on clustering with spatial constraints is developed. Such adaptive quantization enables us to represent the high frequency subbands at low bit rate without losing clinically useful information. The preliminary results of analysis and synthesis show that, by combining the wavelet decomposition with the adaptive quantization, the volumetric biomedical images can be coded at low bit rate while still preserving the desired details of biomedical structures.

Several compression schemes are currently under investigation to code the adaptively quantized high frequency subbands. These schemes aim at taking advantage of two major characteristics of the processed high frequency subbands: (1) well structured directional edges due to separable wavelet filters, and (2) large homogeneous regions due to clustering with spatial constraints. With the reduced entropy, these high frequency subbands can be coded at much lower bit rate than the original subbands.

Acknowledgement

The authors wish to thank Professor W. Li of the Lehigh University, who kindly provided us a 2D version of the subband analysis and synthesis programs, and Mr. J. Luo of the University of Rochester, who offered help in some of the programming.

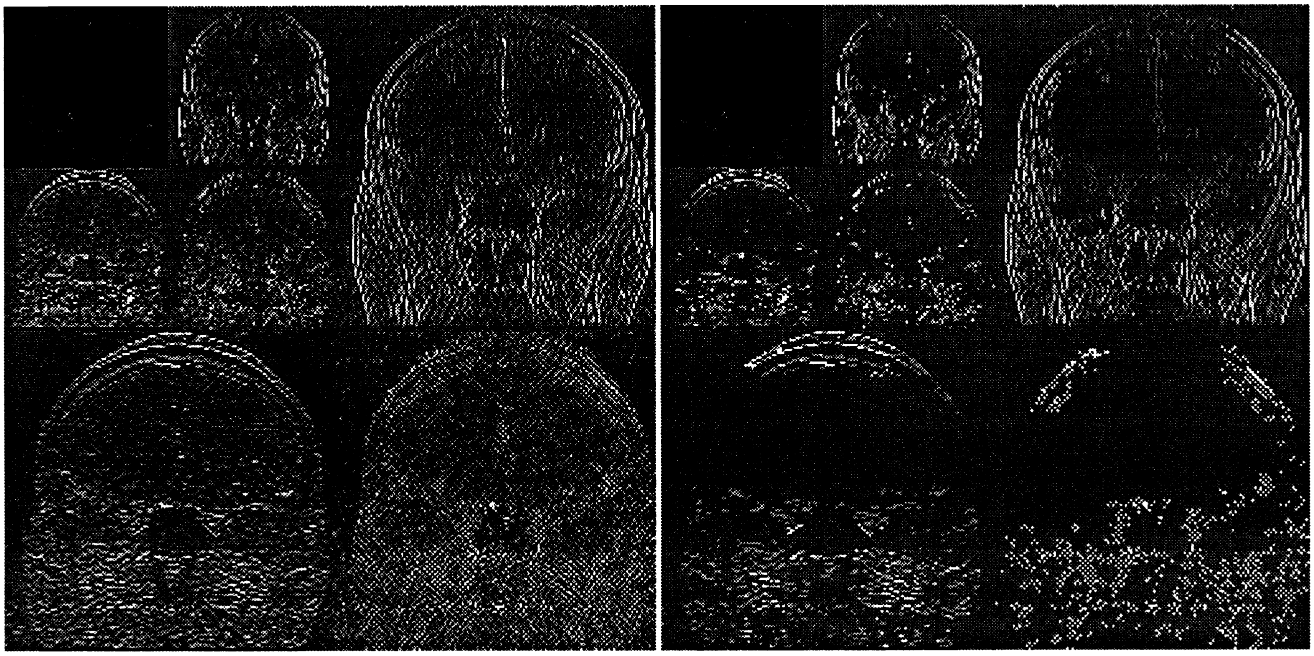

Figure 3: Left: The decomposed 12th slice (resulted from original slice 45, 46, 47, 48) from the octree structure of the decomposed volume; Right: The same slice after the adaptive quantization.

Table 1 A comparison of entropy for each subband presented in Figure 3 .

	Original Decomposition			After Adaptive Quantization		
Subbands	0th order	1st order	DPCM	0th order	1st order	DPCM
LHL	3.94	3.65	4.76	1.57	1.33	2.41
LLH	4.12	3.93	4.41	0.94	0.85	1.11
LHH	2.85	2.61	3.69	0.66	0.59	1.03
LLL-LHL	4.35	3.99	5.05	1.40	1.31	2.24
LLL-LLH	4.41	4.08	4.79	1.35	1.25	1.79
LLL-LHH	3.85	3.63	4.49	1.08	1.05	1.55
Average Entropy:	3.92	3.65	4.53	1.17	1.06	1.67
	Average Entropy Reduction :			70%	71%	65%

References

[1] O. Rompelman, "Medical image compression: possible application of subband coding," in *Subband Image Coding* (J. W. Woods, ed.), pp. 319–352, Boston, MA: Kluwer Academic Publishers, 1991.

[2] A. Bist, A. Jacquin, and C. Podilchuk, "Encoding of the chrominance signals in 3D subband-based video coding," in *Proc. International Conf. Acoustics, Speech and Signal Processing*, (Minneapolis, MN), pp. V–329–332, 1993.

[3] C. Podilchunk and A. Jacquin, "Subband video coding with a dynamic bit allocation and geometric vector quantization," in *Human Vision, Visual Processing, and Digital Display III*, vol. SPIE 1666, (Boston, MA), pp. 241–252, 1992.

[4] M. Antonini, M. Barlaud, P. Mathieu, and I. Daubechies, "Image coding using vector quantization in the wavelet transform domain," in *Proc. International Conf. Acoustics, Speech and Signal Processing*, pp. 2297–2300, 1990.

[5] M. Antonini, M. Barlaud, P. Mathieu, and I. Daubechies, "Image coding using wavelet transform," *IEEE Trans. Image Processing*, vol. 1, pp. 205–220, 1992.

[6] T. Pappas, "An adaptive clustering algorithm for image segmentation," *IEEE Trans. Signal Proc.*, vol. 40, pp. 901–914, 1992.

[7] S. Geman and D. Geman, "Stochastic relaxation, Gibbs distribution, and the Bayesian restoration of images," *IEEE Trans. Patt. Anal. Machine Intell.*, vol. 6, pp. 721–741, 1984.

[8] R. E. Crochiere, S. A. Webber, and J. L. Flanagan, "Digital coding of speech in subbands," *Bell System Technical Journal*, vol. 55, pp. 1069–1985, 1976.

[9] M. Vetterli, "Multi-dimensional subband coding: some theory and algorithms," *Signal Processing*, vol. 6, pp. 97–112, 1984.

[10] J. W. Woods and S. D. O'Nell, "Sub-band coding of images," *IEEE Trans. Acoustics, Speech and Signal Processing*, vol. 34, pp. 1278–1288, 1986.

[11] H. Gharavi and A. Tabatabai, "Subband coding of monochrome and color images," *IEEE Trans. Circuits and Systems*, vol. 35, pp. 207–214, 1988.

[12] P. H. Westerink, J. Biemond, D. E. Boekee, and J. W. Woods, "Subband coding of images using vector quantization," *IEEE Trans. Communication*, vol. 36, pp. 713–719, 1988.

[13] G. Karlsson and M. Vetterli, "Three dimensional sub-band coding of video," in *Proc. International Conf. Acoustics, Speech and Signal Processing*, pp. 1110–1113, 1988.

[14] J. Hartung, "Architecture for the real-time implementation of three-dimensional subband video coding," in *Proc. International Conf. Acoustics, Speech and Signal Processing*, (San Francisco, CA), pp. III–225–228, 1992.

[15] C. Podilchunk, N. S. Jayant, and P. Noll, "Sparse codebooks for the quantization of non-dominant subbands in image coding," in *Proc. International Conf. Acoustics, Speech and Signal Processing*, (Albuquerque, NM), pp. 2101–2104, 1990.

[16] N. Mohsenian and N. M. Nasrabadi, "Subband coding of video using edge-based vector quantization technique for compression of the upper bands," in *Proc. International Conf. Acoustics, Speech and Signal Processing*, (San Francisco, CA), pp. III–233–236, 1992.

[17] O. Johnsen, O. V. Shentov, and S. K. Mitra, "A technique for the efficient coding of the upper bands in subband coding of images," in *Proc. International Conf. Acoustics, Speech and Signal Processing*, (Albuquerque, NM), pp. 2097–2100, 1990.

[18] H. Gharavi, "Subband coding of video signals," in *Subband Image Coding* (J. W. Woods, ed.), pp. 229–272, Boston, MA: Kluwer Academic Publishers, 1991.

[19] H. Derin and H. Elliot, "Modeling and segmentation of noisy and textured images using gibbs random fields," *IEEE Trans. Patt. Anal. Machine Intell.*, vol. 9, pp. 39–55, 1987.

[20] S. Lakshmanan and H. Derin, "Simultaneous parameter estimation and segmentation of gibbs random fields using simulated annealing," *IEEE Trans. Patt. Anal. Machine Intell.*, vol. 11, pp. 799–813, 1989.

[21] J. Besag, "Spatial interaction and the statistical analysis of lattice system," *Journal of the Royal Statistical Society*, vol. 36, pp. 192–326, 1974.

[22] M. M. Chang, A. M. Tekalp, and M. I. Sezan, "Bayesian segmentation of MR images using 3D Gibbsian priors," in *Image and Video Processing* (M. Rabbani, M. I. Sezan, and A. M. Tekalp, eds.), vol. 1903, San Jose, CA: SPIE, February 1993.

[23] J. Besag, "On the statistical analysis of dirty pictures," *Journal of the Royal Statistical Society*, vol. 48, pp. 259–302, 1986.